Low-Field Magnetic Domain Wall Motion and Mobility in CoFeB Nanostripes Influenced by The Dzyaloshinskii-Moriya Interaction

Raditya Nugraha[1], Candra Kurniawan[2], Adam Badra Cahaya[1], Dwiria Wahyuni[3], & Dede Djuhana[1,*]

[1]Department of Physics, FMIPA Universitas Indonesia, Kampus UI Depok, Depok 16424, Indonesia
[2]Research Center for Energy Materials, National Research and Innovation Agency (BRIN), KST B.J. Habibie, Tangerang Selatan, 15314, Indonesia
[3]Department of Physics, FMIPA Universitas Tanjungpura, Pontianak 78124
*E-mail: dede.djuhana@sci.ui.ac.id

Abstract. This work examines the effects of the Dzyaloshinskii–Moriya interaction (DMI) on low-field magnetic domain wall (DW) dynamics in perpendicular anisotropy CoFeB nanostripes driven by nanosecond magnetic field pulses. Micromagnetic simulations based on the Landau–Lifshitz equation were performed for DMI strengths from 0 to 1 mJ m^{-2} and pulse amplitudes of 0.1 to 1 mT, which are commonly regarded to be within the creep regime. The results show that DMI significantly enhances DW displacement and velocity, with a velocity enhancement of up to approximately eight times higher than in the absence of DMI, primarily due to the emergence of a chiral Néel wall configuration and an effective DMI field that increases DW mobility. However, this enhancement does not scale linearly with DMI strength. Instead, both velocity and displacement exhibit a clear saturation behavior beyond intermediate DMI values (~0.6 mJ m^{-2}). Mobility analysis, obtained by fitting simulation results to an analytical DW velocity model, indicates an increase of up to two orders of magnitude with DMI, followed by a similar plateau. These findings highlight a limit to DMI-induced enhancement in the low-field regime, with implications for optimizing DW-based spintronic devices.

Keywords: *CoFeB; DMI; magnetic domain wall; micromagnetics; perpendicular magnetic anisotropy.*

1 Introduction

Interest in magnetic domain wall (DW) dynamics has remained high throughout the years, as it is a pivotal part of the development of state-of-the-art spintronic devices such as racetrack memory, magnetic tunnel junction (MTJ), and magnetoresistive random-access memory (MRAM) [1–5]. In recent years, DW

Received June 15th, 2026, Revised September 16th, 2026, Accepted for publication September 22th, 2026
Copyright © 2026 Published by ITB Institute for Research and Community Service, ISSN: 2337-5760, DOI: 10.5614/j.math.fund.sci.2026.58.1.3

dynamics studies have expanded beyond in-plane magnetization anisotropy (IMA) nanostrips and thin films. Researchers have begun studying a variety of materials, including perpendicular magnetization anisotropy (PMA) ferromagnets and antiferromagnets [6–10]. In the past decade, DW dynamics studies have also begun to incorporate the Dzyaloshinskii-Moriya interaction (DMI), which is an asymmetric exchange interaction often observed in ferromagnet/non-magnet multilayer systems [11–13]. The presence of DMI is known to influence DW dynamics in several aspects, such as enhancing its velocity, suppressing the Walker breakdown, and facilitating stable magnetic topologies such as skyrmions and chiral Néel walls [14–17].

In the low-field regime, DMI-influenced DW dynamics is a well-understood phenomenon and is often used experimentally to measure DMI's strength [18,19]. However, most studies in this regime used a continuous field to drive the DW instead of a nanosecond pulse. Using field pulses to drive a DW is known to have several advantages over a continuous field, such as higher Walker fields and lower joule heating [20,21]. Thus, combining the implementation of DMI with field-pulse driven DW motion may result in an even more advantageous DW motion. Through micromagnetic simulations, we examined how DMI affects the low-field DW dynamics in PMA CoFeB nanostripes when driven by nanosecond field pulses. Similar to DW motion in higher fields, the DW velocity was enhanced. This enhancement can be explained by the DMI effective field (H_{DMI}) influencing the DW mobility. Interestingly, the DW velocity enhancement noticeably plateaus as DMI strength increases. This indicates that there might be a limit to the DW velocity enhancement in the low field instead of steadily increasing linearly.

2 Micromagnetic Simulation

The model used for the simulations is shown in Figure 1. It consists of a rectangular CoFeB nanostripe with a length (L), width (W), and thickness (T) of 1000, 50, and 1 nm, respectively. The material parameters are representative of an ultrathin $Co_{40}Fe_{40}B_{20}$ film with PMA taken from the study of Wang et al. [22]. The exact parameter values used were as follows: saturation magnetization, M_s = 8.75×10^5 A/m, exchange stiffness constant A = 1×10^{-11} J/m, and uniaxial anisotropic constant $K_u = 7 \times 10^5$ J/m^3. The DMI strength for this study varied between D = 0.2 and 1 mJ m^{-2} in steps of ΔD = 0.2 mJ m^{-2}. This is in range with commonly observed DMI strengths for multilayers with CoFeB thin films as their ferromagnetic layer [19]. Experimentally, DMI strength can be tuned by several methods, such as tuning the ferromagnet thickness [23], interface irradiation [24,25], or using different non-magnetic layers like W, Pt, or Ta [26,27]. The nanosecond field-pulse amplitude was varied from 0.1 to 1 mT. Micromagnetic simulations were performed using the Object Oriented Micromagnetic

Framework (OOMMF) software [28]. The software performs micromagnetic calculations based on the Landau-Lifshitz (LL) equation:

$$\frac{d\boldsymbol{M}}{dt} = -|\gamma|\boldsymbol{M} \times \boldsymbol{H}_{eff} - \frac{|\gamma|\alpha}{M_s}\boldsymbol{M} \times (\boldsymbol{M} \times \boldsymbol{H}_{eff}) \quad (1)$$

where γ is the gyromagnetic ratio constant given by $2.21 \times 10^5\ m/As$ and α is the Gilbert damping constant and is set to 0.1. Calculations were performed on a grid of discretized cubic cells of the sample with the dimension of these cells set to 2 × 2 × 1 nm³. This cell dimension was determined to be smaller than the calculated exchange length, which is roughly $l_{ex} = \sqrt{\frac{2A}{\mu_0 M_s}} = 4.56\ nm$. DMI was incorporated using the package developed by Rohart and Thiaville [29], which is suitable for systems assuming that DMI originates at interfaces in ultrathin ferromagnetic layers.

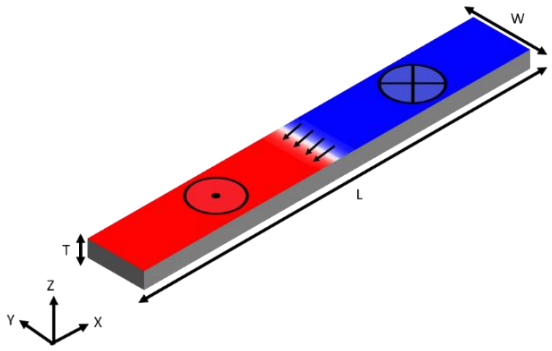
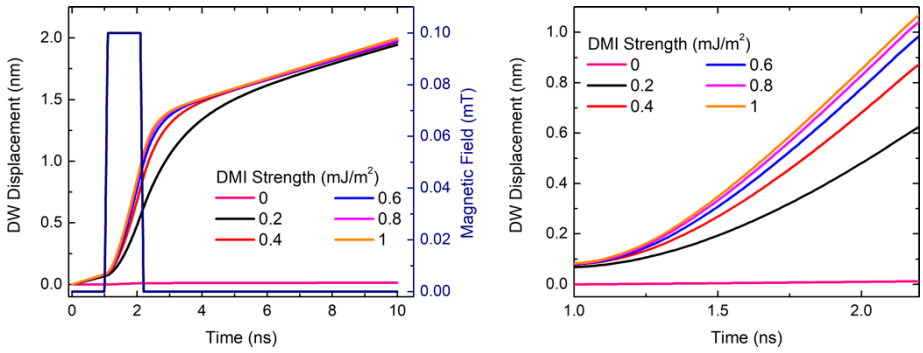


Figure 1 Nanostripe model used in the simulations.

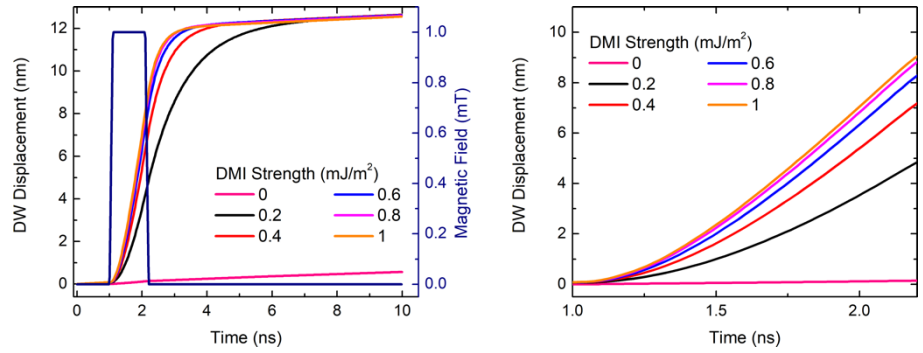
The nanostripe was initialized with a Bloch-type domain wall (DW) located at its center, oriented along the +y direction as its ground-state. Upon implementing the DMI, the magnetization was relaxed without an external field to account for the newly introduced effective DMI field (H_{DMI}) effects on the DW ground-state configuration. During this relaxation process, the ferromagnetic energy reached a new minimal ground-state energy, with the Bloch-type DW transforming into a chiral Néel-type DW aligned along the -x direction, as illustrated with the black arrows of Figure 1. The transition is expected, as the applied DMI strength exceeds the critical D value for CoFeB, given by $D_C = \frac{4\Delta K}{\pi} \sim 0.01\ mJ\ m^{-2}$ [14]. Consequently, the Néel-type DW becomes the new ground-state configuration for simulations that include DMI. Every simulation was started with a 1 ns relaxation period (0 to 1 ns). The applied nanosecond field pulse, which is a square pulse, was then applied along the +z-axis (H_z), with identical rise and fall times of 0.1 ns. The simulation was then kept running for roughly 10 ns.

From the obtained simulation data, the DW position along the x-direction can be calculated by multiplying the normalized, volume-averaged z-component of magnetization (M_z/M_s), whose positive value being the magnetization facing away from the page, by the nanostripe's half-length (500 nm). The DW velocity of each pulse amplitude and DMI strength was obtained by calculating the slope of the position over time curve. This velocity evaluation was restricted to the time interval corresponding to the pulse peak, namely 1.1 to 2.1 ns.

3 Results and Discussion



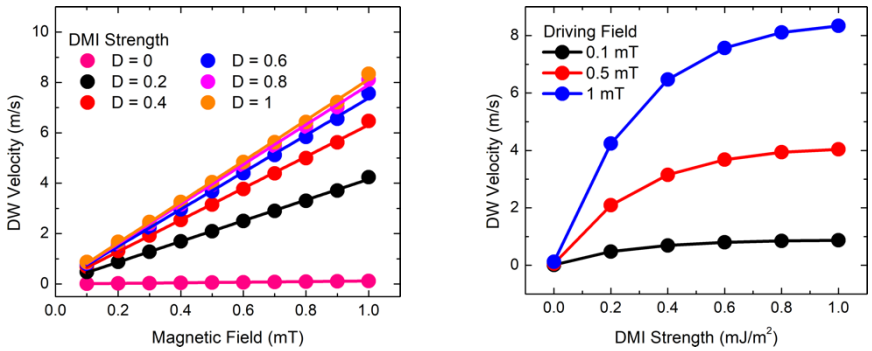
(a)



(b)

Figure 2 Plots of the DW displacement over time in the presence of different DMI strengths driven by a (a) 0.1 and (b) 1 mT nanosecond field pulses. The left panels show the plots of the DW displacement for its entire simulation time, while the right panels show zoomed-in plots of the DW displacement focusing on the active field pulse duration of 1 ns from 1 to 2 ns.

Figure 2 shows detailed DW displacement graphs over time for a 0.1 mT and 1 mT nanosecond field pulse. The DW displacement was measured from the initial relaxed DW position of each DMI strength. DW motion enhancement by DMI was observed and the DW could move up to ten times farther than without DMI. This enhancement may be due to newly added contributions to the magnetostatic energy and an effective local field caused by DMI's presence, which allows the DW to move faster and farther during the active pulse [30,31]. The DMI can also influence the DW motion post-nanosecond-pulse application, leading to a more rapid deceleration. This phenomenon has been observed in a previous study in which DW deceleration became faster with increasing DMI strength [32]. Interestingly, the DW motion enhancement appeared to saturate above a certain threshold, as seen in the zoomed-in (right-side) DW displacement graph of Figure 2. Above a certain DMI strength (D = 0.6 to 1 mJ/m^2), the DW motion begins to converge, as opposed to moving faster as DMI strength increases. This saturation in enhancement may be related to how stronger DMI also affects the Walker breakdown in higher fields. The presence of sufficiently strong DMI is known to cause continuous Bloch-line nucleation and annihilation around the Walker breakdown field [15,33]. In lower fields, it is possible that although the Bloch-lines do not nucleate, the presence of DMI is still able to divert the energy that was meant to drive the DW, leading to a saturation of the DW velocity enhancement.



(a) (b)

Figure 3 (a) DW velocity versus nanosecond field amplitude for varying DMI strengths; (b) DW velocity versus DMI strength for the 0.1, 0.5, and 1 mT driven DW motion.

We now analyze DMI's influence on the low-field DW velocity. Figure 3(a) shows a plot of the low-field (0.1 to 1 mT) DW velocity versus the applied field amplitude for each DMI strength. In addition to the expected linear velocity

increase with respect to the applied field, DW velocity enhancement up to a maximum of roughly eight times faster for the strongest DMI case ($D = 1$ mJ m^{-2}) can be observed. Interestingly, the DW velocity enhancement appears to saturate/converge as DMI strength increases. This is better observable in Figure 3(b), which shows a plot of the DW velocity versus DMI strength for DW motion driven by the 0.1, 0.5, and 1 mT field pulse. Figure 3(b) indicates that for a given field amplitude, the DMI-induced DW velocity enhancement is not linear. It instead plateaus as the DMI strength increases. This may be a consequence of the fact that DMI mainly enhances the maximum DW velocity (Walker velocity) and Walker field instead of an overall DW motion enhancement.

DMI is known to enhance the Walker velocity and Walker field linearly following the equation [31]:

$$v_w \approx \frac{\pi\gamma D}{2\mu_0 M_s} \qquad H_w \approx \alpha \frac{\pi D}{2\mu_0 M_s \Delta} \tag{2}$$

where μ_0 is the permeability of free space and Δ is the DW width. Although DMI affects both Walker velocity and field linearly, it is possible that this exact linear relation is also the reason why the DW velocity enhancement is not linear below the Walker field. In order for the Walker velocity and field to be linear with increasing DMI, it stands to reason that the DW velocity below the Walker field may not necessarily follow the same linear enhancement.

We next analyze the low-field DW mobility to further investigate DMI's role in the low-field DW velocity enhancement. We do this by comparing and then fitting the low-field DW velocity of Figure 3(a) with the analytical DW velocity equation given by [31,34]:

$$v = \frac{|\gamma|\Delta}{\alpha} H_{appl} \tag{3}$$

where H_{appl} is the applied field amplitude and $\frac{|\gamma|\Delta}{\alpha}$ is also known as the DW mobility (μ). Figure 4 shows a modified plot of Figure 3(a), with the addition of the analytical DW velocity calculated with Equation 3. Calculations using Equation 3 resulted in DW velocity values slightly higher than the extracted DW velocities from the simulations. This is to be expected, since Equation 3 typically assumes a steady-state velocity under a continuous driving field. Meanwhile, the simulation DW velocities were extracted from the instantaneous nanosecond field pulse motion, leading to noticeably slower velocities.

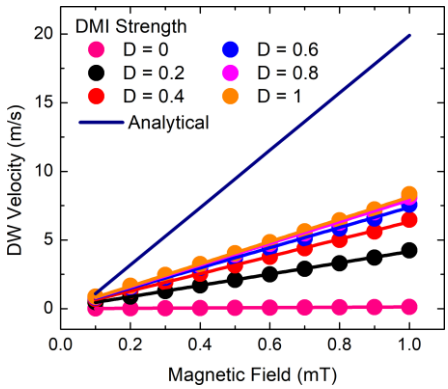


Figure 4 DW velocity versus nanosecond field amplitude for varying DMI strengths and the non-DMI analytical DW velocity calculated using Equation 3.

By fitting the extracted DW velocities with Equation 3 and obtaining the fitted slope, we can analyze and estimate DMI's numerical influence on the DW mobility. This is done by modifying the DW mobility equation:

$$\mu = \mathrm{d}\,\frac{|\gamma|\Delta}{\alpha} \tag{4}$$

where d is an added proportionality constant obtained by substituting μ with the obtained fitting slope. Table 1 shows the values of the obtained fitting slope for each DMI strength, their corresponding standard error, and the d values calculated using Equation 4. Figure 5 shows a plot of the calculated d values with respect to the DMI strength. Interestingly, the calculated d values for all DMI strength variations are all in the same 10^{-4} range. This indicates that the presence of DMI can increase DW mobility by at least two orders of magnitude compared to without DMI. The order of magnitude for the calculated d values also leads us to believe that this proportionality constant may be related to the effective field acting upon the ferromagnet. For the calculated values with DMI, d may be related to the internal DMI field (H_{DMI}), while for the value without DMI, d may be related to both the demagnetization and the anisotropy fields. The calculated d values also appear to plateau as the DMI strength increases, similar to DW velocity for a given applied field plateau with increasing DMI strength. This may serve as further evidence that DW velocity enhancement in the low-field regime or for a given applied field value is not linear and instead follows an exponential enhancement with respect to DMI strength.

Table 1 Values of the fitted slope for each DMI strength, their corresponding standard error, and the d values calculated using Equation 4.

DMI Strength (mJ m^{-2})	Fitted Slope	Standard Error	Calculated d Value
0	0.12042	0.00167	5.8×10^{-6}
0.2	4.11012	0.04041	1.967×10^{-4}
0.4	6.28848	0.07424	3.009×10^{-4}
0.6	7.35818	0.09133	3.521×10^{-4}
0.8	7.88909	0.09959	3.775×10^{-4}
1	8.11333	0.10302	3.882×10^{-4}

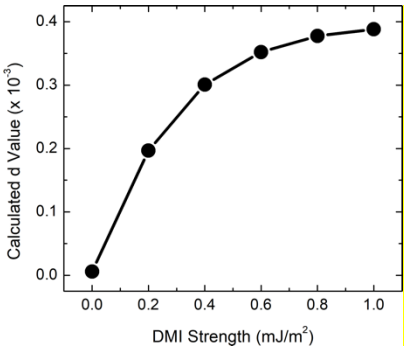


Figure 5 Plot of the calculated d values with respect to DMI strength.

4 Conclusion

We performed micromagnetic simulations to examine the effect of DMI on the low-field DW dynamics in CoFeB nanostripes. We found that DMI can enhance the DW velocity up to eight times further than without DMI in the low-field regime. We also found that DMI-induced DW motion enhancement in the low-field regime or for a given field value is not linear, unlike DMI's enhancement on both the Walker velocity and field. This is evidenced by the exponential rise

of the DW velocity with respect to DMI strength and the obtained mobility proportionality constant, which also plateaus as DMI strength increases. These findings may influence future low-field DMI applications in spintronic devices, as the DW motion enhancement seem to converge with stronger DMI. Further research involving other materials and experimental or simulation approaches could be carried out to confirm the general applicability of these results.

Acknowledgement

This work was funded by the Hibah Dana Padanan FMIPA UI – FMIPA UNTAN Year 2025 No. PKS-50/UN2.F3.D/PPM.00.02/2025 through DRPM Universitas Indonesia.

References

[1] Hirohata, A., Sukegawa, H., Yanagihara, H., Zutic, I., Seki, T., Mizukami, S. & Swaminathan, R., *Roadmap for Emerging Materials for Spintronic Device Applications*, IEEE Transactions on Magnetics, **51**(10), 2015. https://doi.org/10.1109/TMAG.2015.2457393.

[2] Parkin, S., *Racetrack Memory: A High Capacity, High Performance, Non-volatile Spintronic Memory*, 2022 IEEE International Memory Workshop (IMW), pp. 6-9, 2022. https://doi.org/10.1109/IMW52921.2022.9779286.

[3] Raymenants, E., Bultynck, O., Wan, D., Devolder, T., Garello, K., Souriau, L., Thiam, A., Tsvetanova, D., Canvel, Y., Nikonov, D.E., Young, I.A., Heyns, M., Soree, B., Asselberghs, I., Radu, I., Couet, S. & Nguyen, V.D., *Nanoscale Domain Wall Devices with Magnetic Tunnel Junction Read and Write*, Nature Electronics **4**(6)**,** pp. 392-398, 2021. https://doi.org/10.1038/s41928-021-00593-x.

[4] Iwata-Harms, J.M., Jan, G., Serrano-Guisan, S., Thomas, L., Liu, H. Zhu, J., Lee, Y.J., Le, S., Tong, R.Y., Patel, S., Sundar, V., Shen, D., Yang, Y., He, R., Haq, J., Teng, Z., Lam, V., Liu, P., Wang, Y.J., Zhong, T., Fukuzawa, H. & Wang, P.K., *Ultrathin Perpendicular Magnetic Anisotropy CoFeB Free Layers for Highly Efficient, High Speed Writing In Spin-transfer-torque Magnetic Random Access Memory*, Scientific Reports, **9**(1), 19407, 2019. https://doi.org/10.1038/s41598-019-54466-7.

[5] Raymenants, E., Wan, D., Couet, S., Canvel, Y., Thiam, A., Tsvetanova, D., Souriau, L., Asselberghs, I., Carpenter, R., Jossart, N., Manfrini, M., Vaysset, A., Bultynck, O., Van Beek, S., Heyns, M., Nikonov, D.E., Young, I.A., Ghosh, S., Vila, L., Garello, K., Pizzini, S., Nguyen, V.D. & Radu, I.P., *Magnetic Domain Walls: From Physics to Devices*, 2021 IEEE International Electron Devices Meeting (IEDM), pp. 32.3.1-32.3.4, 2021. https://doi.org/10.1109/IEDM19574.2021.9720689.

[6] Fukami, S., Suzuki, T., Ohshima, N., Nagahara, K. & Ishiwata, N.,

Micromagnetic Analysis of Current Driven Domain Wall Motion in Nanostrips with Perpendicular Magnetic Anisotropy, Journal of Applied Physics, **103**(7), 2008. https://doi.org/10.1063/1.2830964.

[7] Dejong, M.D. & Livesey, K.L., *Analytic Theory for The Switch from Bloch to Néel Domain Wall in Nanowires with Perpendicular Anisotropy*, Physical Review B, **92**(21), 214420, 2015. https://doi.org/10.1103/PhysRevB.92.214420.

[8] Albert, M., Franchin, M., Fischbacher, T., Meier, G. & Fangohr, H., *Domain Wall Motion in Perpendicular Anisotropy Nanowires with Edge Roughness*, Journal of Physics: Condensed Matter, **24**(2), 024219, 2012. https://doi.org/10.1088/0953-8984/24/2/024219.

[9] Herranen, T. & Laurson, L., *Bloch-line Dynamics within Moving Domain Walls in 3D Ferromagnets*, Physical Review B, **96**(14), 144422, 2017. https://doi.org/10.1103/PhysRevB.96.144422.

[10] Yang, S.H., Ryu, K.S. & Parkin, S., *Domain-wall Velocities of Up to 750 m s^{-1} Driven by Exchange-coupling Torque in Synthetic Antiferromagnets*, Nature Nanotechnology, **10**(3), pp. 221-226, 2015. https://doi.org/10.1038/nnano.2014.324.

[11] Dzyaloshinskii, I., *A Thermodynamic Theory of "Weak" Ferromagnetism of Antiferromagnet*, Journal of Physics and Chemistry of Solids, **4**(4), pp. 241-255, 1958. https://doi.org/10.1002/pssb.2220460236.

[12] Moriya, T., *Anisotropic Superexchange Interaction and Weak Ferromagnetism*, Physical Review, **120**(1), pp. 91-98, 1960. https://doi.org/10.1103/PhysRev.120.91.

[13] Fert, A., Grünberg, P., Barthélémy, A., Petroff, F. & Zinn, W., *Layered Magnetic Structures: Interlayer Exchange Coupling and Giant Magnetoresistance*, Journal of Magnetism and Magnetic Materials, **140**, pp. 1-8, 1995. https://doi.org/10.1016/0304-8853(94)00880-9.

[14] Thiaville, A., Rohart, S., Jué, É., Cros, V. & Fert, A., *Dynamics of Dzyaloshinskii Domain Walls in Ultrathin Magnetic Films*, Europhysics Letters, **100**(5), 57002, 2012. https://doi.org/10.1209/0295-5075/100/57002.

[15] Yoshimura, Y., Kim, K.J., Taniguchi, T., Tono, T., Ueda, K., Hiramatsu, R., Moriyama, T., Yamada, K., Nakatani, Y. & Ono, T., *Soliton-like Magnetic Domain Wall Motion Induced by the Interfacial Dzyaloshinskii-Moriya Interaction*, Nature Physics, **12**(2), pp. 157-161, 2016. https://doi.org/10.1038/nphys3535.

[16] Mühlbauer, S., Binz, B., Jonietz, F., Pfleiderer, C., Rosch, A., Neubauer, A., Georgii, R. & Böni, P., *Skyrmion Lattice in A Chiral Magnet*, Science, **323**(5916), pp. 915-919, 2009. DOI: 10.1126/science.1166767

[17] Chen, G., Zhu, J., Quesada, A., Li, J., N'Diaye, A.T., Huo, Y., Ma, T.P., Chen, Y., Kwon, H.Y., Won, C., Qiu, Z.Q., Schmid, A.K. & Wu, Y.Z., *Novel Chiral Magnetic Domain Wall Structure in Fe/Ni/Cu(001) Films*,

Physical Review Letters, **110**(17), 177204, 2013. https://doi.org/10.1103/PhysRevLett.110.177204.

[18] Kim, D.H., Kim, D.Y., Yoo, S.C., Min, B.C. & Choe, S.B., *Universality of Dzyaloshinskii-Moriya Interaction Effect Over Domain-wall Creep and Flow Regimes*, Physical Review B, **99**(13), 134401, 2019. https://doi.org/10.1103/PhysRevB.99.134401.

[19] Kuepferling, M., Casiraghi, A., Soares, G., Durin, G., Garcia-Sanchez, F., Chen, L., Back, C.H., Marrows, C.H., Tacchi, S. & Carlotti, G., *Measuring Interfacial Dzyaloshinskii-Moriya Interaction in Ultrathin Magnetic Films*, Reviews of Modern Physics, **95**(1), 015003, 2023 https://doi.org/10.1103/RevModPhys.95.015003.

[20] Sun, Z.Z., & Schliemann, J., *Fast Domain Wall Propagation Under An Optimal Field Pulse in Magnetic Nanowires*, Physical Review Letters, **104**(3), 037206, 2010. https://doi.org/10.1103/PhysRevLett.104.037206.

[21] Kurniawan, C., Djuhana, D., Soegijono, B. & Kim, D.H., *Micromagnetic Investigation of the Sub-nanosecond Magnetic Pulse Driven Domain Wall Motion in CoFeB Nanowire*, Current Applied Physics, **27**, pp. 98-102, 2021. https://doi.org/10.1016/j.cap.2021.04.017.

[22] Wang, Y., Wei, D., Gao, K.Z., Cao, J. & Wei, F., *The Role of Inhomogeneity of Perpendicular Anisotropy in Magnetic Properties of Ultra Thin CoFeB Film*, Journal of Applied Physics, **115**(5), 053901, 2014. https://doi.org/10.1063/1.4863139.

[23] Dohi, T., DuttaGupta, S., Fukami, S. & Ohno, H., *Reversal of Domain Wall Chirality with Ferromagnet Thickness in W/(Co) FeB/MgO Systems*, Applied Physics Letters, **114**(4), 042405, 2019. https://pubs.aip.org/aip/apl/article/114/4/042405/1022895.

[24] Diez, L.H., Voto, M., Casiraghi, A., Belmeguenai, M., Roussigné, Y., Durin, G., Lamperti, A., Mantovan, R., Sluka, V., Jeudy, V., Liu, Y.T., Stashkevich, A., Chérif, S.M., Langer, J., Ocker, B., Lopez-Diaz, L. & Ravelosona, D., *Enhancement of the Dzyaloshinskii-Moriya Interaction and Domain Wall Velocity through Interface Intermixing in Ta/CoFeB/MgO*, Physical Review B, **99**(5), 054431, 2019. https://doi.org/10.1103/PhysRevB.99.054431.

[25] Zhao, X., Zhang, B., Vernier, N., Zhang, X., Sall, M., Xing, T., Diez, L.H., Hepburn, C., Wang, L., Durin, G., Casiraghi, A., Belmeguenai, M., Roussigné, Y., Stashkevich, A., Chérif, S.M., Langer, J., Ocker, B., Jaiswal, S., Jakob, G., Kläui, M., Zhao, W. & Ravelosona, D., *Enhancing Domain Wall Velocity through Interface Intermixing in W-CoFeB-MgO Films with Perpendicular Anisotropy*, Applied Physics Letters, **115**(12), 122404, 2019. https://doi.org/10.1063/1.5121357.

[26] Soucaille, R., Belmeguenai, M., Torrejon, J., Kim, J. V., Devolder, T., Roussigné, Y., Chérif, S.M., Stashkevich, A.A., Hayashi, M. & Adam, J.P., *Probing the Dzyaloshinskii-Moriya Interaction in CoFeB Ultrathin Films*

Using Domain Wall Creep and Brillouin Light Spectroscopy, Physical Review B, **94**(10), 104431, 2016. https://doi.org/10.1103/PhysRevB.94.104431.

[27] Agrawal, P., Büttner, F., Lemesh, I., Schlotter, S. & Beach, G.S.D., *Measurement of Interfacial Dzyaloshinskii-Moriya Interaction from Static Domain Imaging*, Physical Review B, **100**(10), 104430, 2019. https://doi.org/10.1103/PhysRevB.100.104430.

[28] Donahue, M., & Porter, D., *OOMMF User's Guide, Version 1.0*, Interagency Technical Report NISTIR 6376, National Institute of Standards and Technology, Gaithersburg, MD, 1999.

[29] Rohart, S. & Thiaville, A., *Skyrmion Confinement in Ultrathin Film Nanostructures in the Presence of Dzyaloshinskii-Moriya Interaction*, Physical Review B, **88**(18), 184422, 2013. https://doi.org/10.1103/PhysRevB.88.184422.

[30] Ryu, K.S., Thomas, L., Yang, S.H. & Parkin, S., *Chiral Spin Torque at Magnetic Domain Walls*, Nature Nanotechnology, **8**(7), pp. 527-533, 2013. https://doi.org/10.1038/nnano.2013.102.

[31] Camley, R.E., & Livesey, K.L., *Consequences of the Dzyaloshinskii-Moriya Interaction*, Surface Science Reports, **78**(3), pp. 100605, 2023. https://doi.org/10.1016/j.surfrep.2023.100605.

[32] Torrejon, J., Martinez, E. & Hayashi, M., *Tunable Inertia of Chiral Magnetic Domain Walls*, Nature Communications, **7**(1), 13533, 2016. https://doi.org/10.1038/ncomms13533.

[33] Nugraha, R., Kurniawan, C., Kim, D. & Djuhana, D., *The Influence of Dzyaloshinskii-Moriya Interaction (DMI) on the Nanosecond Pulse-driven Domain Wall Dynamics on CoFeB Nanostripe*, Physica Scripta **100**(9), 095931, 2025. https://doi.org/10.1088/1402-4896/ae012e.

[34] Cullity, B.D. & Graham, C.D., *Introduction to Magnetic Materials*, John Wiley & Sons, Inc., 2009. https://doi.org/10.1021/cr2001349.